Wear, 162–164 (1993) 57–63

The performance of aluminium alloys and particulate reinforced aluminium metal matrix composites in erosive–corrosive slurry environments

J. A. Bester and A. Ball

Department of Materials Engineering, University of Cape Town, Private Bag, Rondebosch 7700 (South Africa)

Abstract

A range of aluminium alloys and particulate reinforced aluminium metal matrix composites has been tested in an apparatus which simulates the erosive–corrosive action of a slurry. The slurry used in the investigation is composed of synthetic mine water and silica sand. The corrosion component of the mass loss was found to be an important synergistic factor. The addition of ceramic reinforcement particles to the matrix alloys has a detrimental effect on the slurry erosion resistance.

1. Introduction

Slurry erosion concerns the removal of surface material by impingement of solid erodent particles suspended in a carrier fluid. Areas of concern include the solid–liquid transport in pipelines in the mining, civil and chemical engineering industries, and the dredging of navigable rivers and water-coal slurry spraying in power generation industries. Solid particle erosion of metals occurs by a combination of cutting, gouging, tearing and ploughing mechanisms [1–7]. Hovis *et al.* [6] found for airborne solid particle erosion that the erosion rate is determined by the single impact crater size and the ductility and fracture processes that control the removal of material lips displaced from the impact crater sites by subsequent particle impacts. Relatively few researchers have studied the synergistic effects of mechanical wear and corrosion [8–17]. In a study by Meyer-Rodenbeck *et al.* [8] the abrasive–corrosive wear of some commercial aluminium alloys was studied. The approach taken was to separate the wear variables involved by a repetitive procedure of abrading a specimen and subsequently corroding it. They found that the alloys 5083, 6261 and 7017 exhibited improved wear performances, under conditions of long corrosion coupled with light abrasive intervals, owing to their good corrosion resistances. It is however important to note in the work done by Meyer-Rodenbeck *et al.* that the corrosion product is not being continuously removed by mechanical forces, and thus there is not a continuous generation of a fresh metal surface as is the case for the slurry erosion. Heitz [9] proposed that when the erodent particle energy is sufficient only to account for damage to passive surface layers, allowing the activated, freshly exposed surface of the metal to corrode, then the erosive wear and corrosion rates are of the same magnitude. However when the particle energy is sufficiently great the base metal is preferentially eroded and the attack is mainly erosive wear. Postlethwaite *et al.* [10] proposed that erosion–corrosion in slurry pipelines carrying aerated slurries is under oxygen mass transfer control and dominated by corrosive metal loss. The slurry erosion prevents the formation of a complete oxide film, that normally protects the surface by stifling the diffusion of oxygen [10]. Using cathodic protection to separate the mechanical wear from that due to the electrochemical processes, El-Raghy *et al.* [11] concluded that most of the weight loss is due to mechanical forces under less corrosive conditions, but that electrochemistry plays a major role in more aggressive environments.

Solid particle erosion of aluminium and aluminium metal matrix composites (MMCs) have been studied extensively [18–23]. Two basic mechanisms were identified for the slurry erosion of MMCs by Turenne and Fiset [18] namely matrix cutting and reinforcement fracture. According to Goretta *et al.* [21] the reduced erosion resistance of MMCs is due to the lack of ductility and matrix constraint caused by reinforcing particles in the MMCs. In erosion tests carried out by Srinivasan *et al.* [22] on a series of Al–4% Cu MMCs containing up to 30vol.% alumina fibres, the erosion rates were found to increase significantly with increasing fibre content. Wilson and Ball [23] studied the airborne

0043-1648/93/$6.00

solid particle erosion of two aluminium alloys (Al2014 and Al6061) reinforced with 10, 15, and 20vol.% alumina particulates; the erosion rates increased with increasing particulate additions. The increasing erosion rates were attributed to the ductility constraints imposed by the increasing reinforcement contents.

The contribution of the reinforcing particles to the corrosion requires study since the mismatch of the electrochemical potential between the matrix and the reinforcement provides a local cell when immersed in an aqueous solution [24, 25]. Sun *et al.* [26] found that the degree of corrosion in SiC reinforced aluminium 6061 alloy in NaCl solutions increased with increasing SiC content. In a study of the corrosion behaviour of silicon carbide particle reinforced 6061 alloy composites, Bhat *et al.* [27] found that corrosion damage of the composites was mainly localised in contrast to the uniform corrosion observed for the base alloy. The composites were found to corrode faster than the base alloy even though the attack was mainly confined to the interface, resulting in crevices or pits. This was attributed to the presence of a thin layer of reaction product present at the interface acting as an effective cathode which when continuous would increase the cathode to anode ratio enabling higher localised corrosion. Thermal problems have a detrimental effect on MMC properties because both the particulates and the aluminium alloy possess different thermal properties. This difference may result in high residual stresses and high dislocation densities at the interfaces after heat treating cycles which may affect both the thermodynamics and kinetics of corrosion [24, 25] as well as slurry erosion performance.

The aim of the present study is to utilise weight loss and electrochemical techniques to investigate the effect of slurry erosion and erosion–corrosion on aluminium alloys and aluminium metal matrix composites.

2. Experimental details

A slurry jet erosion apparatus, based on that of Zu *et al.* [7], was developed which permits the effects of the impact angle, erodent size, erodent concentration, velocity, temperature and the carrier fluid parameters to be changed. The apparatus allows the individual and synergistic effects of slurry erosion and corrosion to be studied. Distilled or synthetic mine water, containing sulphates (715 ppm) and chlorides (350 ppm), is pumped at 55 °C from a holding tank into an ejector. The resulting pressure differential draws up a concentrated erodent-fluid mixture from a funnel shaped bed of 500 μm silica sand. The dilute slurry thus formed in the ejector leaves the 4.5 mm diameter exit nozzle horizontally at 8.5 m s^{-1} to impact the specimen at 90°. After impact the sand particles fall back into the funnel, leaving the carrier fluid free of erodent to be recirculated. The impact velocity is derived from the measured cross-sectional area of the exit nozzle and the volume of slurry collected in a known time period. The particle weight concentration is determined by weighing a known volume of collected slurry and may be adjusted by varying the geometry of the ejector. A slurry concentration of 10% by mass was used for all the tests. The test specimens are discs 4 mm thick and 15.7 mm in diameter which have been polished to a 1 μm finish. The test specimens are cleaned ultrasonically in alcohol, weighed, tested, cleaned again ultrasonically in alcohol and then weighed for mass loss, the reproducibility of these results has been found to be within 5%. Using this procedure the material's slurry erosion rate expressed in microgram of target removed per gram of impacting particles is determined.

A specimen holder was developed to permit *in situ* electrochemical measurements to be made. The circuit used for the electrochemical measurements is shown in Fig. 1. The sample holder exposes 1 cm^2 of the specimen face and accommodates the various electrodes. A platinum wire which serves as the counter-electrode encircles the specimen opening. The reference electrode, a saturated calomel electrode (SCE), is placed in a holder arranged outside the specimen chamber, and is connected to the system by an electrolyte bridge. The working electrode makes contact with the back of the specimen.

During the test procedure the corrosion potential of the specimen is monitored continuously against time. For the first 60 min of this test the specimen is exposed to the slurry jet, for the next 60 min of the test the erodent is removed from the impacting fluid jet by shortening the suction tube, so that it does not reach into the sand bed. For the last 10 min the erodent is again added to the impacting fluid jet in order to achieve the steady state eroded surface to facilitate microstructural examination.

In a further supplementary electrochemical test procedure, a potential scan was applied to the specimen in order to obtain its current density *vs.* potential curves. The polarisation of the alloy starts at -2000 mV (SCE) and ends at 1500 mV. This ensures that the potential scan starts 500 to 1200 mV more negative than the alloy's rest (corrosion) potential.

3. Results

The performance of the different matrix alloy materials were evaluated in distilled and synthetic mine water, both with and without the erodent particles, in an attempt to separate the erosion and corrosion components. Table 1 gives a ranking of slurry erosion and

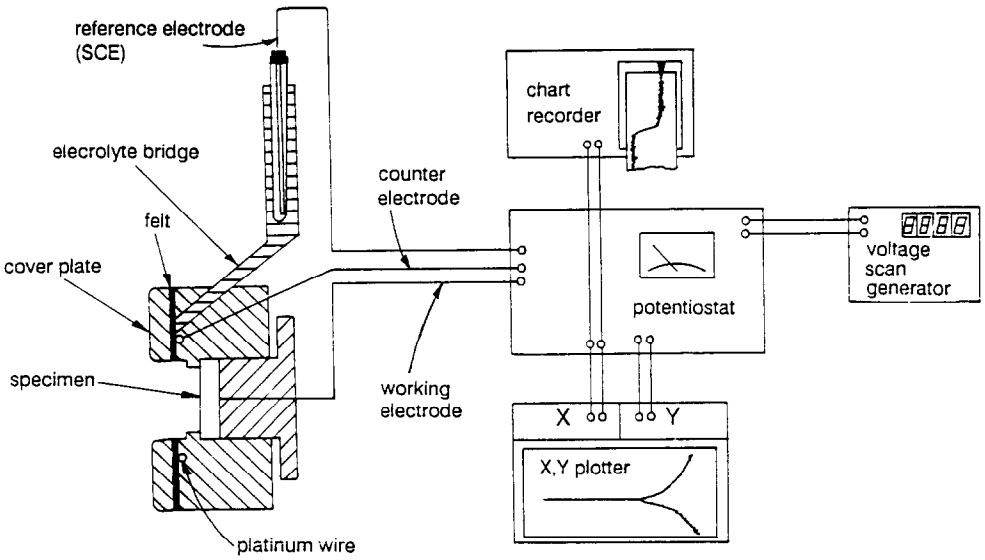

Fig. 1. The arrangement for the electrochemical measurements.

TABLE 1. Slurry erosion rates and corrosion current (i_{corr}) values in distilled water and synthetic mine water. The increments in slurry erosion rates due to the presence of mine water are also tabulated

Distilled water				Synthetic mine water			
Alloy	Hardness (HV20)	Erosion rate ($\mu g\ g^{-1}$)	i_{corr} (nA cm^{-2})	Alloy	Erosion rate ($\mu g\ g^{-1}$)	i_{corr} ($\mu A\ cm^{-2}$)	Erosion rate increase ($\mu g\ g^{-1}$)
Al1200	31	0.477	70	Al1200	0.676	200	0.199
Al3004	52	0.423	80	Al7017	0.545	200	0.129
Al7017	136	0.416	80	Al3004	0.544	300	0.121
Al2014	151	0.396	30	Al2014	0.516	200	0.120
Al5083	104	0.396	90	Al6261	0.499	200	0.116
Al6261	123	0.383	50	Al5083	0.460	50	0.064

erosion–corrosion resistance together with the hardness and measured corrosion current, i_{corr}, values of the matrix alloys.

Figures 2 and 3 show the single impact sites on the 5083 series alloy specimen tested in distilled water containing 5 g of silica sand particles.

The results in Table 1 show that in general the heat-treatable aluminium alloys (2014, 6261 and 7017) have lower slurry erosion rates than the non-heat-treatable alloys tested (1200 and 3004); the non-heat-treatable 5083 alloy being an exception. Note that the rankings of the materials when subjected to the synthetic mine water do not change significantly, although all the materials do show a significant increase in slurry erosion rates due to the corrosion media. The 5083 series alloy which showed the smallest increase in slurry erosion rate also has an i_{corr} markedly smaller than that of any of the other alloys. For all the materials tested the current density increases by at least three orders of magnitude when tested in the synthetic mine water as opposed to distilled water (Figs. 4 and 5).

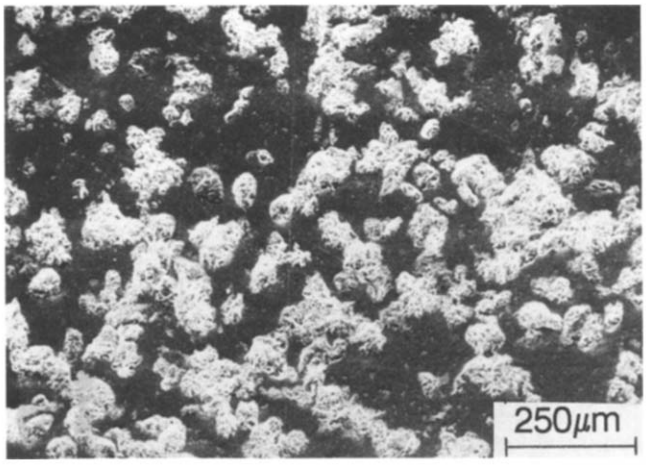

Fig. 2. Single impact sites on a polished Al5083 surface tested in distilled water containing 5 g of silica sand particles.

The values of the corrosion current densities are also greater when measured during slurry erosion than when measured only in the fluid jet; the curves in Figs.

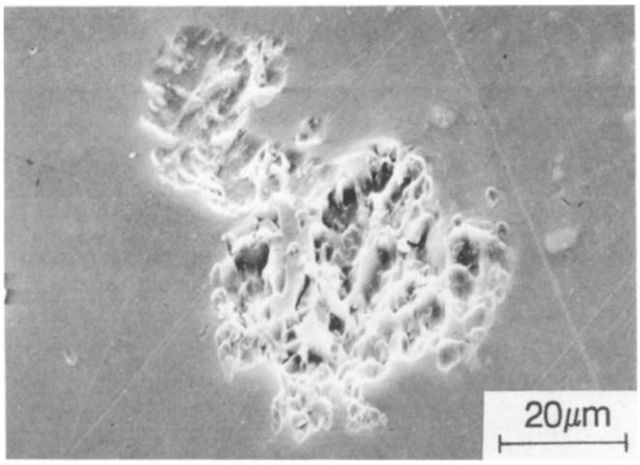

Fig. 3. A single impact site on a polished Al5083 surface tested in distilled water.

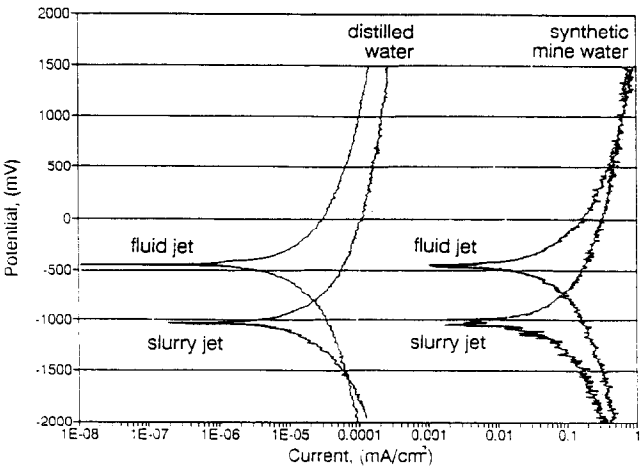

Fig. 4. Al2014 – graphs of the current density *vs.* potential scans: abrasive, silica sand (500 μm); carrier fluid, distilled water and synthetic mine water (pH 5.7); temperature, 55 °C; impact angle, 90°; rate of polarisation 2 mV s^{-1}.

4 and 5 shift to the right when subjected to slurry erosion by the silica sand. The current density *vs.* potential curves of the 2014 series alloys presented in Fig. 4 illustrate the general trends observed for the alloys. Note however that only in the case of the 5083 aluminium alloy (Fig. 5) when eroded in the synthetic mine water slurry, was any passivation observed.

It can be seen from the potential *vs.* time curves of the 5083 series alloy, presented in Fig. 6, that during the initial 20 min of the test there is a gradual drop in potential, with the rest potential becoming gradually more negative until a steady state is reached. There is a distinct change in the rest potential after the first 60 min, when only the carrier fluid is left to impinge on the surface. After approximately 70 min of testing in the synthetic mine water, the potential gradually becomes less negative (Fig. 6). This is not observed when tested in distilled water.

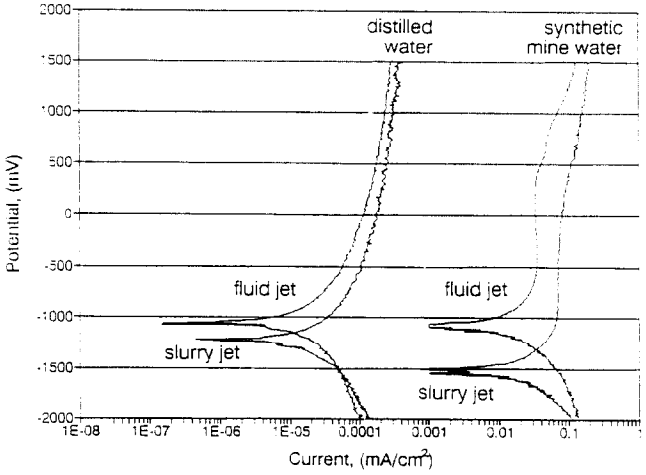

Fig. 5. Al5083 – graphs of the current density *vs.* potential scans: abrasive, silica sand (500 μm); carrier fluid, distilled water and synthetic mine water (pH 5.7); temperature, 55 °C; impact angle, 90°; rate of polarisation 2 mV s^{-1}.

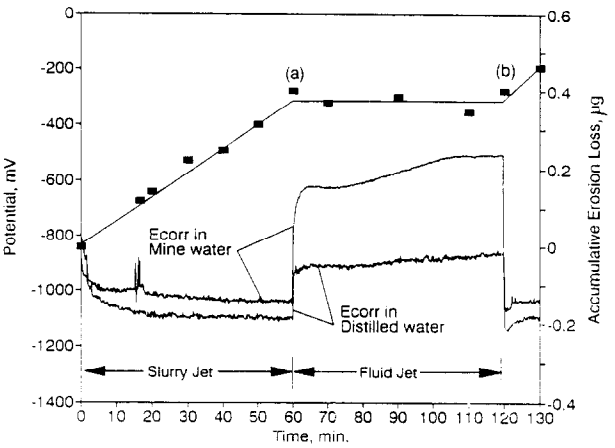

Fig. 6. The potential *vs.* time curves of the 5083 aluminium alloy, tested in distilled water and synthetic mine water at 55 °C with 500 μm silica sand as abrasive, are presented with the accumulative slurry erosion loss measurements of the 5083 series alloy tested in synthetic mine water.

Scanning electron microscopy (SEM) images of the steady state eroded surfaces of the 5083 series alloy are presented in Figs. 7(a) and 7(b); these are typical of the steady state conditions of all the alloys tested. Figure 7(a) illustrates the eroded surface after the first 60 min of the test and Fig. 7(b) illustrates the surface after 120 min, these correspond respectively to points (a) and (b) on the graph in Fig. 6. The cutting due to individual impact events (Fig. 7(a)) is more visible after 60 min of slurry erosion than after a further 60 min of corrosion in the synthetic mine water jet.

Note that there was no measurable mass loss when the 5083 alloy was only subjected to the synthetic mine water fluid jet (Fig. 6). As a control a polished 5083 series alloy was tested for 60 min in only the mine water carrier fluid jet; there was no apparent mass loss.

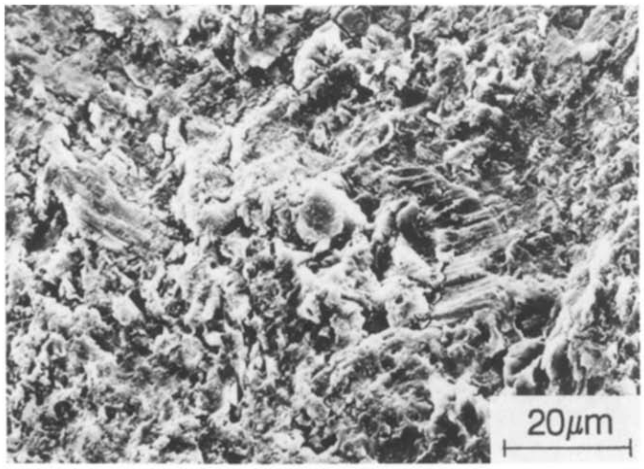

(a)

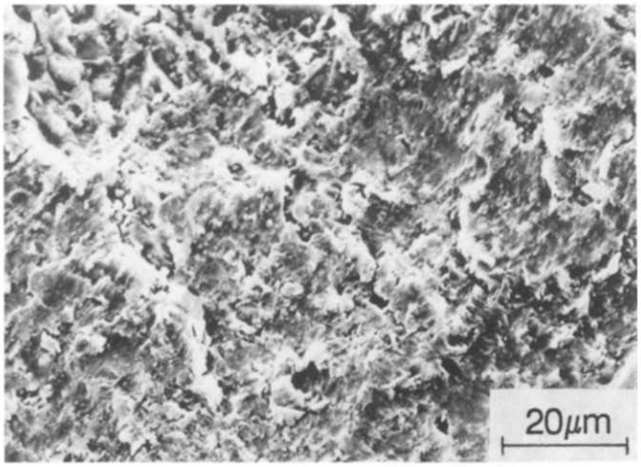

(b)

Fig. 7. SEM images of the 5083 series alloy after (a) 60 min of slurry erosion–corrosion and (b) a further 60 min of corrosion.

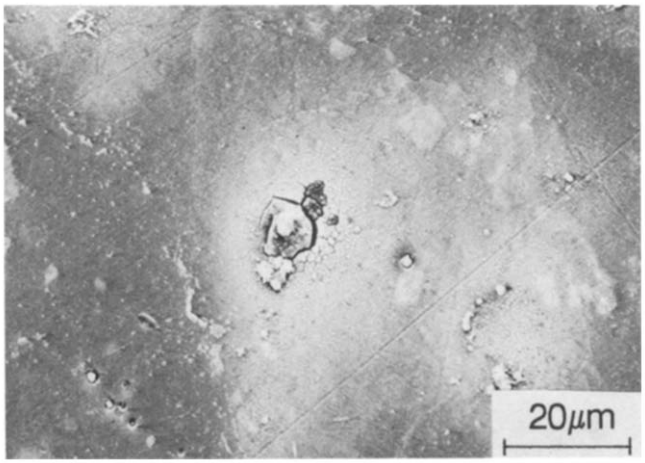

Fig. 8. The corrosion attack on a polished Al5083 surface after 60 min of corrosion in the synthetic mine water jet.

TABLE 2. The results of the slurry erosion tests performed in synthetic mine water, on the MMCs and their constituent alloys. The work to fracture results obtained by Wilson and Ball [23] are also tabulated

Alloy	Volume fraction	Particulate diameter (μm)	Hardness (HV20)	Erosion rate (μg g^{-1})	Work to fracture (Mpa)
Al2014	0	–	151	0.516	49.9
Al2014	15%Al_2O_3	13.6	174	0.555	5.42
Al2014	20%Al_2O_3	27.2	197	0.551	2.23
Al6061	0	–	124	0.469	33.92
Al6061	15%Al_2O_3	15.1	135	0.556	24.15
Al6061	20%Al_2O_3	32.2	152	0.605	8.25

The SEM image, Fig. 8, shows preferential corrosion of the solid solutionaround particle constituents as well as a breakdown of the surrounding oxide layer.

The MMCs investigated comprised two different aluminium alloys, namely 2014 and 6061, reinforced with alumina particulates. Each composite and matrix alloy was received in the extruded state having been solution treated and artificially aged to peak hardness (T6). The results of the tests performed on the MMCs and their constituent alloys are presented in Table 2. The composites eroded more rapidly than did the base alloys, despite their greater hardness values.

4. Discussion

The lower slurry erosion rates of the heat-treatable aluminium alloys as opposed to the non heat-treatable alloys (Table 1), are similar to results found previously [8]. In the abrasion tests performed by Meyer-Rodenbeck *et al.* [8], the non-heat-treatable wrought alloys were found to exhibit ductile micro-deformation characteristics, whilst heat-treatable alloys had the best dry abrasion resistance values, owing to their better combinations of strength hardness and toughness. Hovis *et al.* [6] found that an alloy's ability to accumulate strain, (its work hardening capacity) improves its erosion resistance.

The increase in current density associated with the increased slurry erosion rates experienced in the synthetic mine water over the distilled water, illustrate the significance of the corrosion component when coupled with slurry erosion. The material loss increased by as much as 40% in the case of the 1200 aluminum alloy (Table 1) when eroded in the presence of synthetic mine water instead of distilled water. The aluminium 1200 alloy is generally known to be corrosion resistant, owing to the rapid formation of a continuous protective oxide layer, but this layer is being continuously damaged and removed by the erodent particles, resulting in the

high slurry erosion losses experienced. The slurry erosion rate of the 5083 series alloy, when tested in the synthetic mine water, increased by only 16%, its I_{corr} value being considerably less than that of any of the other matrix alloys. The 5083 alloy however shows signs of passivation, but only when tested in the synthetic mine water due to the driving force provided by the corrosive medium. The insignificant corrosion losses measured for the 5083 series alloy is consistent with the weight losses recorded by Meyer-Rodenbeck *et al.* [8] for the 5083 series alloy after three 48 h periods of corrosion in flowing synthetic mine water. Meyer-Rodenbeck *et al.*'s results also showed that as corrosion becomes the more predominant wear factor in an abrasive–corrosive wear environment, overall wear resistance is determined primarily by the corrosion properties of the series of alloys, whilst the dry abrasion properties of individual alloys within that series becomes less important. Meyer-Rodenbeck *et al.* [8] found that the corrosion attack on the aluminium alloys is not uniform, but is confined to localised sites on the metal surface where heterogeneity of either the metal or the corrosive medium exists and passivation is discontinuous. In the case of aluminium alloys, the most common form of corrosive attack is localised corrosion or pitting. However under slurry erosion conditions the surface is constantly changing and hence localized conditions are not allowed to develop. This is illustrated by the fact that the rest potential gradually decreases, at the start of each potential *vs.* time test (Fig. 6), owing to the gradual breakdown of any existing passive film. The decrease in potential also occurs owing to the increase in surface area brought about by the slurry erosion. The increase in corrosion current that occurs when an erodent is present in the fluid jet is due to the continuous generation of fresh material owing to the slurry erosion by the silica sand particles and a passive oxide is prevented from forming.

The addition of the ceramic reinforcement to each alloy was found to result in a reduction in erosion resistance (Table 2); similar results were obtained by Wilson *et al.* [23] and were found to relate to the strain energy required to initiate micro-fracture in a material. This is related to the area beneath a material's tensile load-extension curve and is an indication of its toughness or work to fracture. Both the Al2014 and the Al6061 composite materials displayed good correlations between their erosion rates and work to fracture values [23]. The composites with small fracture energies exhibited rapid material losses, as opposed to the unreinforced alloys having the greatest fracture energy values and minimal erosion losses [23].

The protrusion of the particulates on the surface are expected to make the formation of a coherent passivating layer difficult, thus further decreasing the resistance of the composites to erosion–corrosion.

5. Conclusions

Slurry erosion can cause extensive metal loss in aluminium alloys and aluminium MMCs. The effect of corrosion alone is insignificant, but the combined action of the slurry erosion and corrosion mechanisms result in a mutual or synergistic reinforcement of their effects. The corrosion current densities, tested under slurry erosion conditions, provides an accurate reflection of the effect of corrosion on the erosion–corrosion performance. Under the conditions tested the addition of reinforcement to the matrix alloys was deleterious to their slurry erosion performance.

Acknowledgments

This research forms part of a collaborative programme with Hulett Aluminium of South Africa. In particular Dr. T. Hurd and Mr. B. I. Dennis are thanked for their support and interest.

References

1 C. M. Preece and N. H. Macmillan, *Ann. Rev. Mater. Sci., 7* (1977) 95–121.
2 A. W. Ruff and S. M. Wiederhorn, *Treat. Mater. Sci. Tech., 16* (1979) 69–126.
3 G. Sundararajan, A comprehensive model for the solid particle erosion of ductile materials, *Wear, 149* (1991) 111–127.
4 I. Finnie and D. H. McFadden, *Wear, 48* (1978) 18.
5 I. G. A. Bitter, *Wear, 6* (1963) 5, 169.
6 S. K. Hovis, J. Talia and R. O. Scattergood, Erosion mechanisms in aluminium and Al–Si alloys, *Wear, 107* (1986) 175–181.
7 J. B. Zu, I. M. Hutchings and G. T. Burstein, Design of a slurry erosion test rig, *Wear, 140* (1990) 331–344.
8 G. D. Meyer-Rodenbeck, T. Hurd and A. Ball, On the abrasive-corrosion wear of aluminium alloys, *Wear, 154* (1992) 305–318.
9 E. Heitz, *Corrosion, 47* (1991) 135–145.
10 J. Postlethwaite, M. H. Dobbin and K. Bergevin, The role of oxygen mass transfer in the erosion–corrosion of slurry pipelines, *Corrosion, 42* (1986) 514–521.
11 S. M. El-Raghy, H. Abd-El-Kader and M. E. Abou-El-Hassan, Electrochemistry of abrasion corrosion of low alloy steel in 1% NaCl solution, *Corrosion, 40* (1984) 60–61.
12 E. Wandke, M. Möser and S. Tscherny, The influence of corrosion and hydrogen cracking on blast wear in wet media, *Wear, 121* (1988) 15–26.
13 B. Poulsen, Electrochemical measurements in flowing solutions, *Corros. Sci., 23* (1983) 391–430.
14 G. A. Gehring, Jr. and M. H. Peterson, *Corrosion, 37* (1981) 232–242.
15 G. T. Burstein and R. J. Cinderey, The potential of freshly generated metal surfaces determined from the guillotined electrode – A new technique, *Corros. Sci., 32* (1991) 1195–1211.
16 R. E. Noël and A. Ball, On the synergistic effects of abrasion and corrosion during wear, *Wear, 87* (1983) 351–361.

17 K. C. Barker and A. Ball, Synergistic abrasive–corrosive wear of chromium containing steels, *Br. Corros. J., 24* (1989) 222–228.
18 S. Turenne and M. Fiset, Evaluation of abrasive particle trajectories in a slurry jet during erosion of metal matrix composites, *Wear Testing of Advanced Materials Symposium,* San Antonio, TX, November 14, 1990.
19 S. Turenne, Y. Châtigny, D. Simard, S. Caron and J. Masounave, The effect of abrasive particle size on the slurry erosion resistance of particulate reinforced aluminium alloys, *Wear, 141* (1990) 147–158.
20 S. Turenne, D. Simard and M. Fiset, Influence of structural parameters on the slurry erosion resistance of squeeze-cast metal matrix composites, *Wear, 149* (1991) 187–197.
21 K. C. Goretta, W. Wu, J. L. Routbort and P. K. Rohatgi, Solid–Particle erosion of aluminium/particulate ceramic composites, in P. K. Rohatgi, C. S. Yust and P. J. Blau (eds.), *Proc. Cong. Tribology of Composite Materials,* Oak Ridge, TN, May 1–3, 1990, ASM International, Materials Park, OH, 1990, pp. 147–155.
22 S. Srinivasan, R. O. Scattergood and R. Warren, Erosion of fibre reinforced Al-4 Pct Cu composites, *Metall. Trans. A, 19A* (1988) 1785–1793.
23 S. Wilson and A. Ball, Performance of metal matrix composites under various tribological conditions, Advances in composite tribology, in K. Friedrich (ed.), *Composite Materials Series* (B. Pipes, ed.), Elsevier, in press.
24 P. P. Trzaskoma, *Corrosion, 42* (1986) 609–613.
25 R. C. Paciej and V. S. Agarwala, *Corrosion, 42* (1986) 718–729.
26 H. Sun, E. Y. Koo and H. G. Wheat, Corrosion behaviour of SiCp/6061 Al metal matrix composites, *Corrosion, 47* (1991) 741–753.
27 M. S. N. Bhat, M. K. Surappa and H. V. Sudhaker Nayak, Corrosion behaviour of silicon carbide particle reinforced 6061/Al alloy composites, *J. Mater. Sci., 26* (1991) 4991–4996.